Journal of Electron Spectroscopy and Related Phenomena, 51 (1990) 149–165
Elsevier Science Publishers B.V., Amsterdam — Printed in The Netherlands

ELECTRON SPECTROSCOPY OF ADSORBATES VIA AUTOIONIZATION OF CORE-TO-BOUND EXCITED STATES: EXPERIMENT AND THEORY

G. ILLING[1], T. PORWOL[1], I. HEMMERICH[1], G. DÖMÖTÖR[1], H. KUHLENBECK[1], H.-J. FREUND[1], C.-M. LIEGENER[2], W. VON NIESSEN[3]

[1]Lehrstuhl für Physikalische Chemie I, Ruhr-Universität Bochum, Universitätsstr. 150, 4630 Bochum, FRG

[2]Institut für Physikalische und Theoretische Chemie, Universität Erlangen-Nürnberg, Egerlandstr. 3, 8520 Erlangen, FRG

[3]Institut für Physikalische und Theoretische Chemie, Technische Universität Braunschweig, Hans-Sommer Str.-10, 3300 Braunschweig, FRG

ABSTRACT

We use autoionization spectroscopy after core-to-bound excitation of adsorbed molecules to get information about the spectral distribution of valence electrons in adsorbates and about the nature of shake up satellite states. Examples are presented for a physisorbed system (CO_2/Ni(110)), a weakly chemisorbed system (N_2/Ni(110)) and a strongly chemisorbed system (CO/Ni(110)). It is shown that in the first case detailed calculations of the autoionization rates of the isolated molecule can basically explain the experimental findings. For N_2/Ni(110) autoionization spectroscopy is shown to verify an assignment put forward for the photoemission spectrum, i.e. that satellites contribute heavily to the valence ionization of many systems. In the third example, the angular dependences of the autoionization lines are used to deduce information on the symmetries of ion states.

1. INTRODUCTION

Photoelectron spectroscopy is a powerful tool for investigating the electronic structure of adsorbed molecules. By analysing binding energies we get information on the nature of the electronic coupling between adsorbed molecules and the substrate, as well as on the nature of intermolecular interactions (1–3). Via angle dependent changes of photoemission intensities the symmetries of the ion state wavefunctions of adsorbed molecules can be determined (1–3). On the other hand, it is very hard to deduce from photoemission direct information on the spatial distribution of electrons in the valence ion states. Also, photoemission has failed so far to allow for detailed spectroscopic investigations of the region of inner valence ionizations of adsorbed molecules. This region appears particularly interesting because here the simple one electron picture of photoemission is known to break down (4), i.e. a whole series of ion states, dominated by two-hole-one-particle configurations (shake-up-states) is expected. Experimentally, strong

0368-2048/90/$03.50

secondary electron emission from the metal substrates swamps the relatively low intense bands due to shake-up states, so that the experimental observation is difficult. Due to these difficulties only very few attempts have been made to

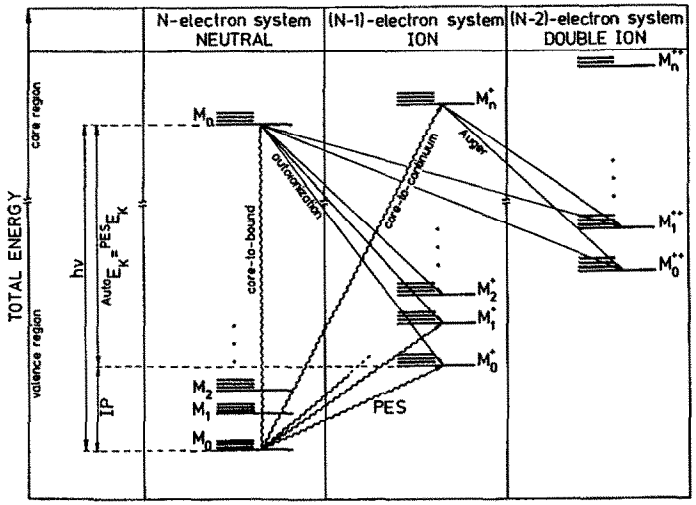

Fig.1: Schematic total energy level diagram for ground and excited states of the neutral N-electron system (left panel), the single hole state N-1-electron system, and the double hole state N-2-electron system. Wiggly arrows indicate photon excitations, straight arrows radiationless decay chanels. The energy scale is broken in order to separate valence- and core-excited states.

investigate the inner valence ionizations of adsorbed molecules by photoelectron spectroscopy (5-7). Several groups have recently chosen a different approach to tackle this problem: electron spectroscopy via autoionization of highly excited states of the adsorbate (8-16). These highly excited states are populated via core-to-bound excitations with synchrotron radiation and radiationless decay into valence ion states of the adsorbate. An energy diagram for these processes is shown schematically in Fig. 1 (second and third panel from the left). If the photoelectron spectrum is recorded with the same photon energy as the autoionization spectrum, the two spectra occur at the same kinetic energies (left panel Fig. 1). Since the two spectroscopic methods probe the same set of ion states it appears natural to put the two sets of electron spectra on the same binding energy scale. We give experimental results for several systems, i.e. physisorbed and chemisorbed molecules on surfaces and, for some examples, compare the experimental spectra with the results of ab-initio calculations including estimates for the autoionization intensities. In the case CO(P2mg)/Ni(110)

we discuss the additional information that can be gained from angle-resolved autoionization spectra.

2. EXPERIMENTAL ASPECTS

The experiments were performed in two different magnetically shielded ultrahigh vacuum systems containing facilities for low energy electron diffraction (LEED), Auger spectroscopy (AES), residual gas analysis with a quadrupole mass spectrometer, and photoelectron spectroscopy. The resolution was typically 1 eV. Excitation of photoelectrons was achieved by synchrotron radiation from the exit slit of a high-energy toroidal grating monochromator (TGM) attached to the storage ring BESSY in Berlin. The base pressure in the system was below 10^{-7} Pa. The Ni(110) and Ni(100) crystals were spot-welded to two tungsten rods on a sample manipulator. With liquid nitrogen the crystal could be cooled to 85 K. Heating was possible by electron impact onto the reverse side of the crystal. The surface was cleaned by argon ion bombardment. After annealing the cleanliness was checked with AES, and surface order and geometry were established by LEED. CO_2, NO_2, NO and CO adsorption was monitored via NEXAFS spectra. Only in the case of CO adsorption was a sharp (2x1) LEED pattern observed.

3. THEORETICAL ASPECTS

To calculate autoionization spectra the binding energies and the ion-state wavefunction need to be known. Both these quantities are calculated via ab-initio or semiempirical Green's function methods. The Green's function calculations are based upon ab-initio SCF or semiempirical calculations and include the effects of electronic correlation and reorganization. In view of the fact that we are particularly interested in the inner valence region we have used the so called extended two-particle-hole Tamm-Dancoff Green's function method (extended 2ph-TDA). This method can be used in the entire valence region and we refer to the literature for details (17).

It has been known for some time (18) that the transition rate for radiationless decay processes, i.e. autoionization and Auger electron emission, is proportional to the square of the expectation value of the Hamiltonian between the initial (Ψ_i) and the final states ($\Psi_f^{(k)}$).

$$I \alpha \sum_k |\langle \Psi_f^{(k)} | H | \Psi_i \rangle|^2 \qquad [1]$$

In the present case the initial state is a core-to-bound excited state, where a 1s-electron has been excited into an unoccupied molecular valence level.

The decay starts by filling the core hole with a valence electron, followed by the emission of a second valence electron. Traditionally, the final state is classified into two categories:

i) the excited electron remains in its orbital while another valence electron decays into the core hole (spectator decay).
ii) the excited electron participates in the decay (direct recombination).

The result of process ii) is a normal single hole state while a double-hole-one-particle (2hp) state is the consequence of the spectator decay i).

To calculate the autoionization spectra involving 2hp-states we have to consider two different cases:
i) both holes reside in the same orbital
ii) both holes reside in different orbitals.

The former case leads to one final doublet state. The latter case gives rise to two possibilities of coupling the spins of the open shells forming the final doublet states. In particular the electron-hole-pair in the 2hp-configuration can be either singlet- or triplet-coupled.
If we describe the initial state, i.e. the core-to-bound state, by a single determinant with spin-orbitals Ψ_k, equation [1] becomes (19):

$$I \alpha \sum_{l,m} |M_{lm}|^2 =$$
$$= \sum_{l,m} |c_1 \langle \Psi_{1s}(1)\Psi_{lm}(2) | 1/r_{12} | \Psi_i(1)\Psi_j(2)\rangle + c_2 \langle \Psi_{lm}(1)\Psi_{1s}(2) | 1/r_{12} | \Psi_i(1)\Psi_j(2)\rangle|^2 \qquad [2]$$

where c_1 and c_2 are constants, Ψ_i and Ψ_j valence orbitals, Ψ_{lm} the continuum orbital, and Ψ_{1s} the 1s core-orbital.
The continuum orbital is chosen in such a way that its angle-dependent part is centered on the hole excited atom and can be described as:

$$\Psi_{lm}(\varepsilon) = R_l(\varepsilon)\, Y_{lm} \qquad [3]$$

where ε is the energy of the outgoing electron and Y_{lm} is the spherical harmonic with quantum numbers lm. We have used the radial integrals of McGuire (20) calculated for the atomic cases.
After a more involved calculation we find the following matrix elements M_{lm} (21):

i) single hole states: $M_{lm} = 2\, J_{lm} - K_{lm}$ [4a]
ii) 2hp states with both holes in the same orbital: $M_{lm} = J_{lm}$ [4b]
iii) 2hp states (singlet coupled): $M_{lm} = 1/\sqrt{2}\ (J_{lm} + K_{lm})$ [4c]
iv) 2hp states (triplet coupled): $M_{lm} = \sqrt{(3/2)}\ (J_{lm} - K_{lm})$ [4d]

with:

$$J_{lm} = \langle \Psi_{ls}\ (1)\ \Psi_{lm}\ (2)\ |1/r_{12}|\ \Psi_i\ (1)\ \Psi_j\ (2) \rangle \qquad [5a]$$

$$K_{lm} = \langle \Psi_{lm}\ (1)\ \Psi_{ls}\ (2)\ |1/r_{12}|\ \Psi_i\ (1)\ \Psi_j\ (2) \rangle \qquad [5b]$$

The molecular orbitals Ψ_k are written as linear combinations of atomic orbitals. This can be used to rewrite the two-electron-orbitals:

$$\Psi_k = \sum_s c_s^k\ \chi_s \quad \text{with } k = i, j \qquad [6]$$

$$J_{lm} = \sum_{r,s} c_r^i\ c_s^j\ \langle \Psi_{ls}(1)\Psi_{lm}(2)|1/r_{12}|\chi_r(1)\chi_s(2)\rangle \qquad [7a]$$

$$K_{lm} = \sum_{r,s} c_r^i\ c_s^j\ \langle \Psi_{lm}(1)\Psi_{ls}(2)|1/r_{12}|\chi_r(1)\chi_s(2)\rangle \qquad [7b]$$

The remaining two-electron orbitals can be calculated employing the so-called one-center-approximation proposed by Siegbahn et al. (22), leading to:

$$J_{lm} = \sum_{l',m'} \sum_{l'',m''} C^{l}_{l'm'} C^{j}_{l''m''} \delta(m'+m'',m) \sum_k c^k(00,l'm')c^k(l''m'',lm)\cdot R^k(10,\varepsilon l,nl'nl'') \qquad [8]$$

and a corresponding one for K_{lm}. The coefficients C^k are well known from literature (23). The above formulae have been programmed.

We have several options to describe the wavefunction of the system after core-to-bound excitation:

i) use the wavefunction of the neutral ground state

ii) use the wavefunction of the system with the localized core-hole ("equivalent-core"-approximation) (24)

So far we have not considered the fact that the emitted electron in the autoionization process exhibits angular dependences. Equation [2] represents the integrated intensity. In order to study the angular dependence of the autoionization current we consider the final state wave function Ψ_f as:

$$\Psi_f = 4\pi \sum_{l,m} i^l \exp(i\beta_l)\ Y_{lm}^*(k)\ \ Y_{lm}(r)\ \ G_{kl}(r) \qquad [9]$$

where k is the unit vector pointing in the direction of the outgoing electron. $G_{kl}(r)$ is the radial part of the wavefunction, and β_l is the phase factor of the l^{th} partially scattered wave (25).

$$\beta_l = \sigma_l\ (\varepsilon) + \delta_l(\varepsilon) \qquad [10a]$$

$$\sigma_l\ (\varepsilon) = \arg\ \Gamma\ (l + 1 - i\ \varepsilon^{-1/2}) \qquad [10b]$$

with Γ = Gamma function.

The methods to calculate $\delta_l(\varepsilon)$ are well etablished and some values are available from literature (26). The differential intensity as a function of angle is now given by:

$$I \alpha |c_1\langle\Psi_{1s}(1)\Psi_f(2)|1/r_{12}|\Psi_i(1)\Psi_j(2)\rangle + c_2\langle\Psi_f(1)\Psi_{1s}(2)|1/r_{12}|\Psi_i(1)\Psi_j(2)\rangle|^2 \quad [11]$$

where Ψ_f is represented by equation [9]. Consequently, equations [4a-d] have to be modified.

$$M_{lm} = (2\,J_{lm} - K_{lm})\;Y_{lm}(\vartheta,\varphi) \quad [12a]$$

$$M_{lm} = J_{lm}\;Y_{lm}(\vartheta,\varphi) \quad [12b]$$

$$M_{lm} = 1/\sqrt{2}\;(J_{lm} + K_{lm})\;Y_{lm}(\vartheta,\varphi) \quad [12c]$$

$$M_{lm} = \sqrt{3}/\sqrt{2}\;(J_{lm} - K_{lm})\;Y_{lm}(\vartheta,\varphi) \quad [12d]$$

In a first very crude approximation we have again used McGuire radial integrals (20) to calculate the matrix elements for angle resolved intensities.

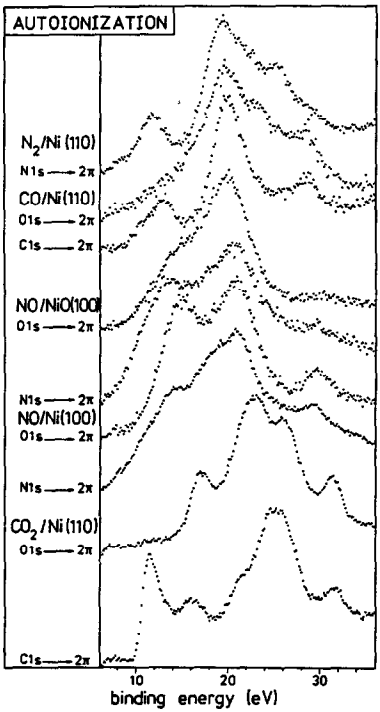

Fig.2 Autoionization spectra of molecular adsorbates on Ni(110) and NiO(100) after core-to-bound excitations of different core electrons.

4. RESULTS AND DISCUSSION

Fig. 2 shows a set of autoionization spectra of various physisorbed and chemisorbed adsorbate systems. Core-to-bound excitations for different core-

electrons in the same system are compared. Note, that there are transitions ranging from below 10 eV to 40 eV binding energies.

The message of Fig. 2 is to demonstrate "by inspection" that autoionization spectra

i) are sensitive to the location of the core-excited atom within the molecular adsorbate, and

ii) show considerable intensity below 14 eV binding energies, where none of the adsorbed molecules show bands in photoemission spectra. Therefore, there is hope that by finally understanding and being able to assign the autoionzation spectra we should be in a position to fill the gap that is left by photoelectron spectroscopy of adsorbates as discussed in the introduction.

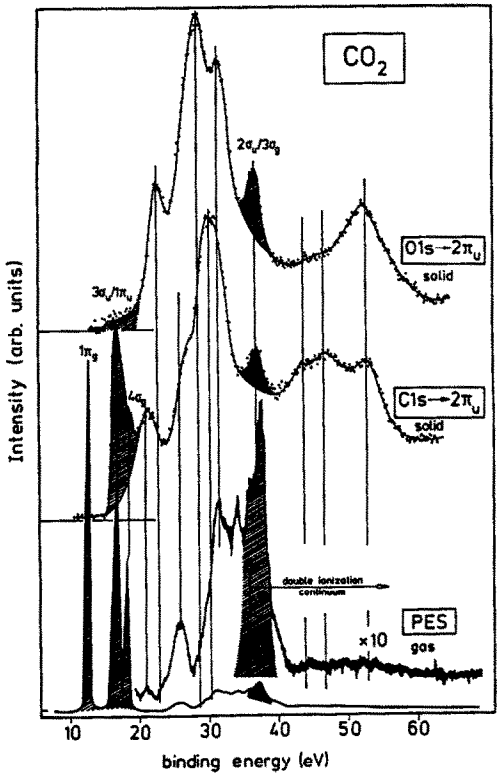

Fig.3: Comparison of the autoionization spectra of physisorbed CO_2 on Ni(110) after C1s→2π and O1s→2π excitation with the gas phase photoelectron spectrum of CO_2. The photoelectron spectrum has been shifted by 0.9 eV to lower binding energies (see text).

In the following we want to elaborate in more detail on three examples out of Fig. 2 in order to demonstrate the potential held by autoionization spectroscopy.
As the first case we consider CO_2 physisorption on Ni(110) which has been studied in detail in the past (27). Fig. 3 shows the autoionization spectra after C1s- (middle) and O1s- (top) to-bound excitation in comparison with the CO_2 gas phase photoelectron spectrum. The autoionization spectra have been shifted by 0.9 eV to lower binding energy to compensate for the well known polarization energy observed for condensed molecular solids in comparision with the gas phase (28).

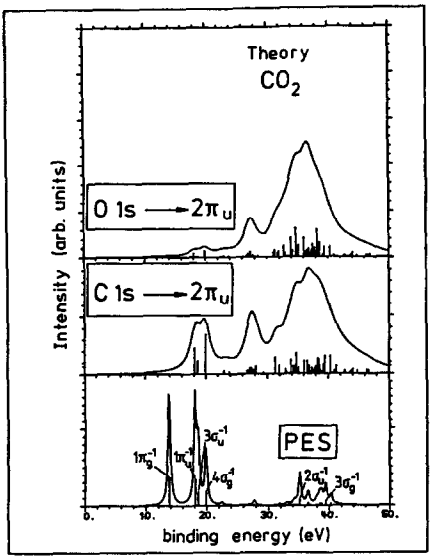

Fig.4: Comparison of the calculated autoionization spectra after C1s→2π and O1s→2π excitation with the calculated photoelectron spectrum of CO_2.

Two effects are striking:

i) The inner valence region, starting below 20 eV binding energy, which exhibits little intensity in photoemission contains the most dominant spectral features in autoionization. The binding energies of the observed features in autoionization can be correlated with binding energies of ion states found in photoemission.

ii) The outer valence region above 20 eV binding energy shows high intensities in photoemission for all ion states. In autoionization the intensity depends on the created core-to-bound states. In the decay of the C1s-to-bound-state, the Πg ion state shows negligible intensity due to its spatial electron distribution. A $1\pi_g$ orbital cannot have electron density on the carbon atom because of symmetry requirements. Therefore the C1s-to-

bound state does not preferentially decay into this state, but rather into those ion states with finite electron density on the carbon atom, namely the $3\sigma_u$, $1\pi_u$ and $4\sigma_g$ states. In the decay of the O1s-to-bound excited state, on the other hand, these symmetry arguments do not hold. Therefore, we expect a finite decay rate into all outer valence ion states. However, the decay rate in this case is very low for the outer valence region so that no definite statement can be made on the basis of the present measurements. The reason for the low intensities is clear: The O1s-to-bound excited state is localized at one end of the CO_2 molecule but decays into outer valence states, where the hole may be rather delocalized. Therefore the overall decay rate decreases considerably.

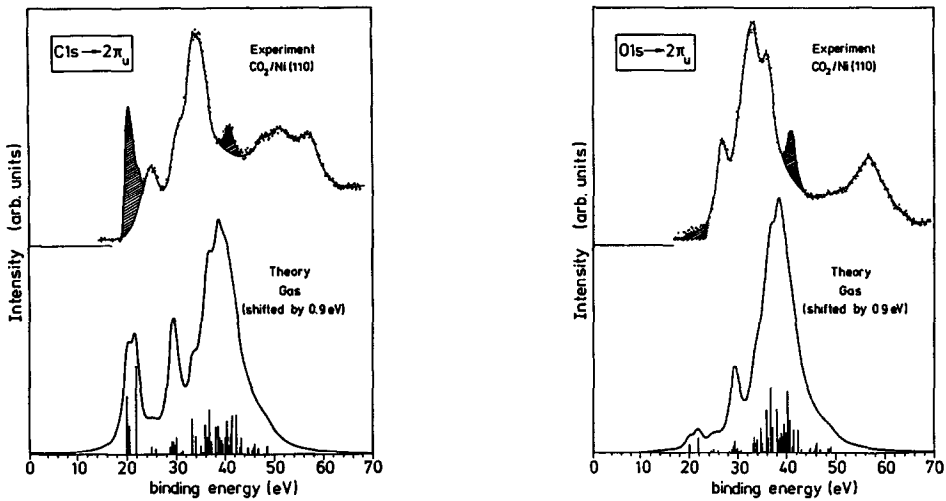

Fig.5: Direct comparison between measured and calculated autoionization spectra after C1s→2π excitation (left panel) and after O1s→2π excitation (right panel). The calculated spectrum has been shifted by 0.9 eV to lower binding energy.

A more or less full account of these observations can be given on the basis of calculations carried out for single CO_2 molecules applying the approximations described in the theoretical part (16). The results of the calculations on the photoelectron and autoionization spectra are shown in Fig. 4 as Lorentzian convolutions of the calculated bar spectra. The details have been discussed in literature (16) and shall not be repeated here, but Fig. 4 shows, in comparison with Fig. 3, that qualitatively the calculation models the experimental observations.

Fig. 5 shows a direct comparison of calculated and experimental spectra and corroborates the above statement. Fig. 5 indicates that the features above 50 eV binding energy are not reproduced by the calculation, because ion states in this energy range have not been considered. Also, these features are situated in the double-ion continuum, so that it is very likely, that they are caused by radiationless transitions between the core-to-bound excited neutral state and double ion outer valence states (16). Such processes are indicated in Fig. 1 by arrows connecting states of the N-electron and the N-2 electron system.

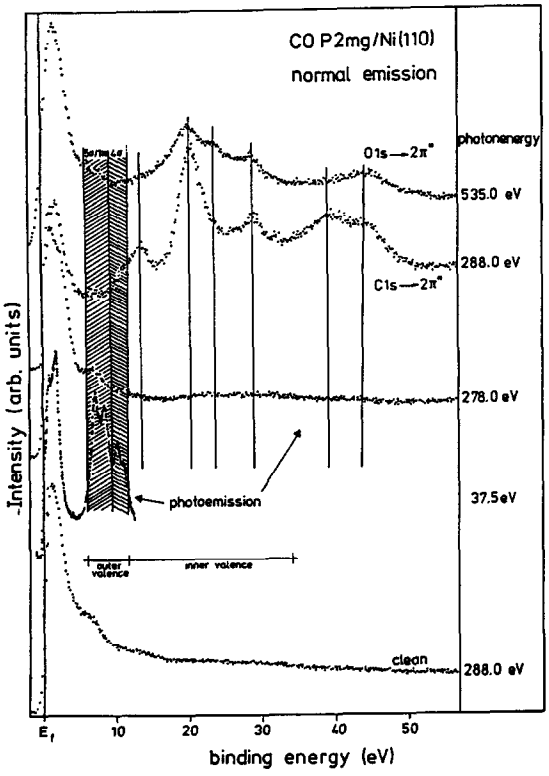

Fig.6: Normal emission electron spectra for various photon energies as indicated. Those spectra taken in resonance with a core-to-bound excitation are marked.

Fig. 6 collects sets of spectra taken for the system CO(2x1)P2mg/Ni(110) (29), an example of a strongly bound adsorbate. Spectrum a) shows the photoelectron spectrum of the clean Ni(110) surface, spectrum b) and c) the photoelectron spectra of the adsorbate system at two different photon energies. The spectrum taken with low photon energy emphasizes the outer valence ion states of the

adsorbates. The σ-derived molecular ion states dominate the spectrum at the chosen photon energy. These states are split pairwise in normal emission due to the glide plane symmetry of the adsorbate, i.e. there are two CO molecules per unit cell tilted by about ~15-20° with respect to the surface normal. The spectrum taken with high photon energy is dominated by the emission of the substrate d-bands, while the outer valence adsorbate bands are very weak. More importantly, however, the spectrum below 15 eV binding energy consists of a structureless background. On the basis of such data it is impossible to identify

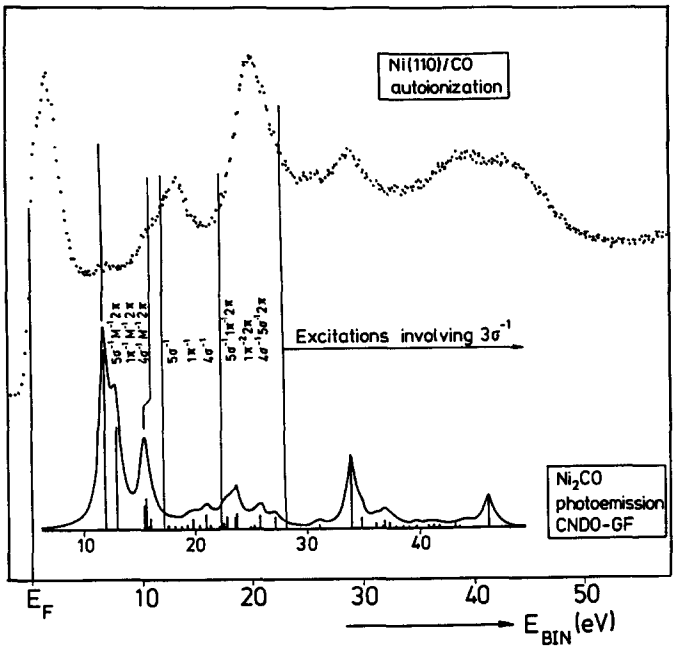

Fig.7: Assignment of the CO(P2mg)/Ni(110) autoionization spectrum after C1s excitation on the basis of a Ni_2-CO cluster calculation.

any specific feature in the inner valence region. The situation changes dramatically when the photon energy reaches the threshold for C1s excitation, i.e. C1s→2π excitation. Spectrum d) represents the corresponding autoionization spectrum. Care has been taken to tune the photon monochromator to the absorption maximum. We are sure that we reside within ±0.2 eV on the C1s→2π maximum. The autoionization spectrum shows little intensity in the outer valence region but rather high intensity in the inner valence region, exhibiting several pronounced maxima. The assignment of these peaks is difficult. One needs calculations of the quality reported for CO_2 (16) in order to find unambiguous

assignments. Such calculations are not available at present. We therefore resort tc semiempirical CNDO based Green's-function calculations on Ni_nCO-cluster reported about a decade ago. Fig. 7 shows a comparison of a calculated photoelectron spectrum and a measured autoionization spectrum. This figure merely serves to show that many of the predicted satellite states in the inner valence region can in fact be found in the spectra.

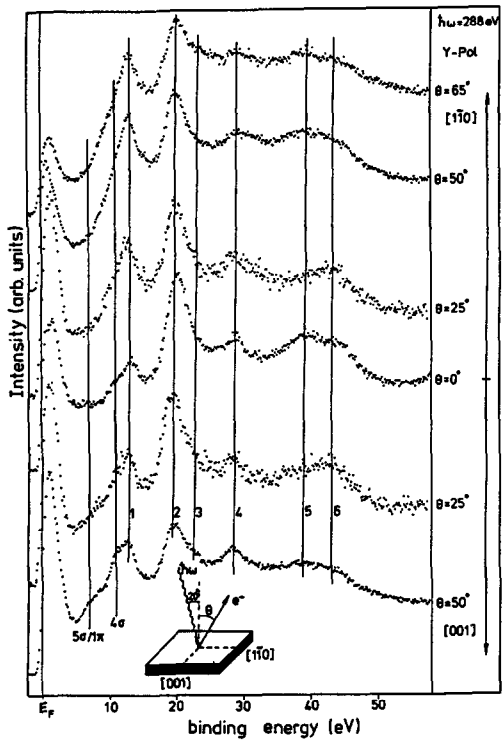

Fig.8: Angle resolved C1s-to-bound autoionization spectra of the system CO(P2mg)/Ni(110) for the (110) and (001) surface azimuths. The light polarization was along the (001) azimuth. The chosen polar angles are indicated in the figure.

In order to assign experimentally the nature, or at least the symmetry of these states, we have several options:

i) We compare the autoionization spectrum after C1s-to-bound excitation (Fig. 6, spectrum c)) with the one after O1s-to-bound excitation (Fig. 6, spectrum d)). There are several changes observed. Firstly, the composite peak at 14 eV binding energy is attenuated, and secondly a feature appears at 24 eV binding energy. Without going into details, which will be done

elsewhere (30), the spectral electron distribution in these states seems to be qualitatively different in the sense that the intensity of the autoionization spectrum samples the degree of spatial localization of the involved valence ion state. How such arguments can be used in detail will be presented in the third example further below.

ii) The angular dependence of the autoionization bands which is conceptually very similar to angle dependent Auger intensities (31) can be used to assign a symmetry to the involved ion state. Fig. 8 shows angular dependences for the above adsorbate along two azimuthes of a Ni(110) surface.

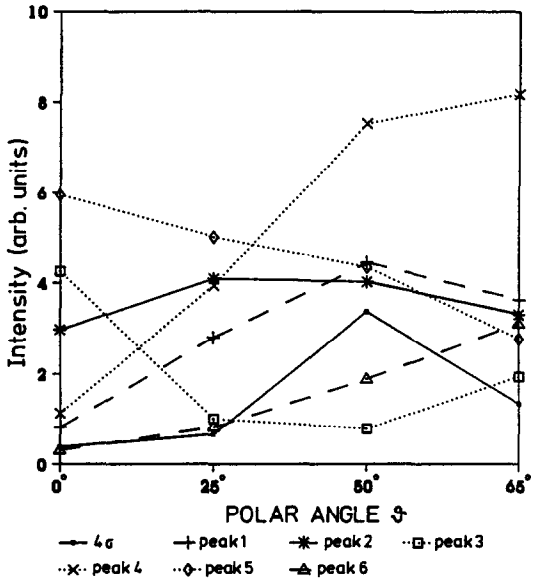

Fig.9: Measured intensities of the autoionization bands as marked in Fig.8 as a function of the polar angle.

In Fig. 9 the variation of the band intensities are determined via curve fitting of the experimental spectra with a minimum set of Lorentzian lines. The various observed angular dependences are remarkable and are in full agreement with the expectations from theoretical considerations outlined in part three.

Fig. 10 shows some calculated angular dependences using the approximations outlined above for some configurations of a free CO molecule (32). These calculations may be compared with experiment for those ion states where we do not expect

extensive participation of metal electrons. This may be the case for the states $4\sigma^{-1}$ or $4\sigma^{-1}\ 5\sigma^{-1}\ 2\pi$. To merely demonstrate the effects expected theoretically,

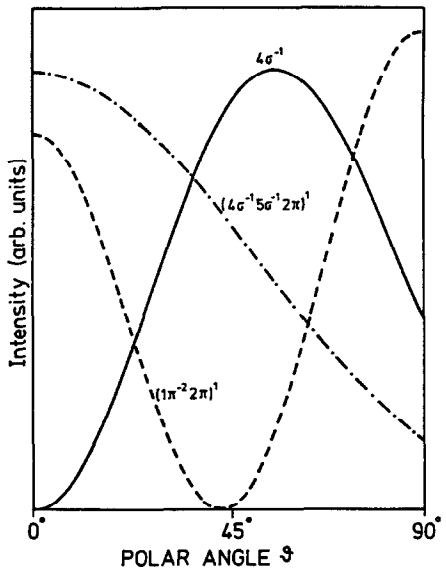

Fig.10: Calculated intensity variations expected for those autoionisation bands with dominating contributions from specific hole- and two-hole-particle states as indicated.

Fig. 7 shows the angular dependences for the above configurations. It basically represents the angular dependence of the square of those spherical harmonics in equation [12] contributing to the particular configuration. It is clear that via the angular dependences different configurations can be differentiated. The $4\sigma^{-1}$ configuration should have its most intense emission at intermediate angles and should have low intensity normal to the surface. The $4\sigma^{-1}\ 5\sigma^{-1}\ 2\pi$ configuration exhibits just the opposite behaviour. As an additional example the $1\sigma^{-2}\ 2\pi$ configuration shows minimal emission current at intermediate polar angles.

The two experimental options outlined provide possibilities of assigning autoionization spectra to an extent that should allow us to get deeper insight into wavefunctions of adsorbed molecules.

The last example, which we shall discuss on the basis of Fig. 11, can be used to illustrate this latter statement in further detail. It is very well known that when the bond strength of a molecule towards the substrate is reduced, the satellite

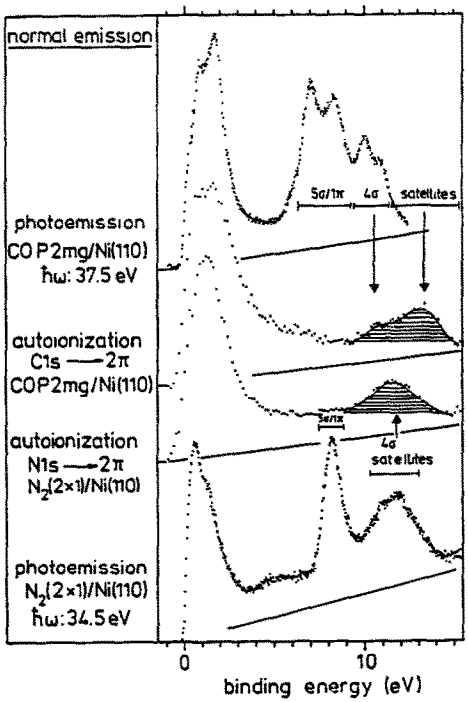

Fig.11: Comparison of normal emission autoionzation and photoemission spectra of the strongly bonded CO-, and a weakly bonded N_2-adsorbate.

lines in the outer valence region become more intense. Photoelectron spectra (33) of the system N_2/Ni(110) have been interpreted in this way some time ago (34). Fig. 11 shows for N_2/Ni(110) in comparison with CO/Ni(110) (29) that autoionization can be successfully used to contribute to a deeper understanding of such phenomena. In the case of CO it is striking to realize that the outer valence σ-ionizations show little, if any, intensity in the autoionization decay. Moreover, 4σ ionizations show up as a shoulder in autoionization, but are rather unpronounced. The peak intensity resides at higher binding energies around 14 eV, where no peak in photoemission can be found if we consider the electronic nature of the ion states involved together with the intensity matrix elements. The dominating peaks in photoemission do not correspond to single hole states (so called "unscreened" states) as in the gas phase, but rather to 2hp-states, where in addition to the creation of a valence hole a metal → CO-2π electron hole pair has been excited. These states are called "screened" states. This leads to configurations of the form:

$V^{-1}M^{-1}2\Pi$ (V^{-1} valence hole; M^{-1} metal hole)

and matrix elements (1):

$$\langle V\Phi_{1m} | 1/r_{12} | M\Phi_{1s} \rangle$$

Had it been a single hole state, the corresponding quantity would be:

$$\langle V\Phi_{1m} | 1/r_{12} | 2\Pi\Phi_{1s} \rangle$$

While in the latter integral, all orbitals are localized on the molecule, in the former, one of the orbitals is located on the metal. This leads to lower intensities in autoionization for those "screened ion states" as compared with "unscreened ion states", and can be verified via the lower part of Fig. 11. For weakly chemisorbed systems, like N_2/Ni(110) we know that especially in the region of the 4σ ionization satellite structures contribute. We can immediately see the consequences in autoionization. We find relatively high intensity in the 4σ region of N_2/Ni(110) as observed in the spectra. Another way of stating this result is: We expect higher autoionization intensitiy for N_2/Ni(110) in comparison with CO/Ni(110) at lower binding energy, opposite to the result in photoemission where we find the 4σ-emission at higher binding energy in N_2/Ni(110). This example indicates that autoionization can help to assign photoelectron spectra in certain cases.

5. SUMMARY AND CONCLUSION

We have demonstrated that autoionization spectroscopy can be used as a complementary method together with photoemission. Autoionization spectroscopy reveals features in the inner valence region of the photoionization of adsorbed molecules. These features can be assigned via angle dependent measurements and on the basis of calculations. If ab-initio calculations are available, a semiquantitative agreement between theory and experiment may be achieved.
The comparison of autoionization spectra after different core-to-bound excitations in the same molecule holds a lot of potential for studying the spatial distribution of valence electrons of adsorbed molecules.

6. ACKNOWLEDGEMENT

The authors thank the Bundesministerium für Forschung und Technologie for financial support of this project under numbers 05363 FAB and 05432 FAB. We are grateful to the Fonds der Chemischen Industrie for funding part of this work.

7. REFERENCES

1 H.-J. Freund, M. Neumann, Appl. Phys. A47, 3 (1988)
2 E.W. Plummer, W. Eberhardt, Adv. Chem. Phys. 49, 533 (1982)
3 N. Richardson, A.M. Bradshaw: in "Electron Spectroscopy" Vol. 4 Ed. C.R. Brundle, A.D. Baker (Academic, New York) 1982.
4 L.S. Cederbaum, W. Domcke, J. Schirmer, W.v. Niessen Adv. Chem. Phys. 65, 115 (1986).
5 J.N. Miller, D.T. Ling, I. Lindem, P.M. Stefan, W.E. Spicer Phys. Rev. Lett. 38, 1419 (1977)
6 H.-J. Freund, F. Greuter, D. Heskett, E.W. Plummer Phys. Rev. B28, 1727 (1983)
7 A. Nilsson, N. Mårtensson to be published.
A. Nilsson, Uppsala University, Uppsala (1988)
8 G. Loubriel, T. Gustafsson, L.I. Johansson, S.J. Oh Phys. Rev. Lett. 49, 571 (1982)
9 C.T. Chen, Thesis, University of Pennsylvania (1985)
10 E.W. Plummer, C.T. Chen, W.K. Ford, W. Eberhardt, R.P. Messmer, H.-J. Freund, Surf. Sci. 158, 58 (1985).
11 W. Eberhardt, Phys. Scri. T17, 28 (1987).
12 D. Menzel, P. Feulner, R. Treichler, E. Umbach, W. Wurth, Phys. Scri. T17, 166 (1987).
13 W. Wurth, C. Schneider, R. Treichler, E. Umbach, D. Menzel Phys. Rev. B35, 7741 (1987).
14 W. Wurth, C. Schneider, R. Treichler, D. Menzel, E. Umbach Phys. Rev. B37, 8725 (1988).
15 G. Illing, T. Porwol, H.-J. Freund, H. Kuhlenbeck, M. Neumann, S. Bernstorff, Prec. 3rd Surf. Sci. Symp. Kaprun, Austria p. 81 (1988)
16 T. Porwol, G. Illing, H.-J. Freund, H. Kuhlenbeck, M. Neumann, S. Bernstorff, W. Braun, W.v. Niessen, C.M. Liegener Phys. Rev. B submitted.
17 J. Schirmer, L.S. Cederbaum, O. Walter, Phys. Rev. A28, 1237 (1983)
18 G. Wenzel, Z. Phys. 29, 321 (1928).
19 T. Åberg, G. Howat in "Handbuch der Physik" Vol 31 "Theory of the Auger Effect" Ed. W. Mehlhorn (Springer, Berlin 1981)
20 E. G. McGuire, Phys. Rev. 185, 185 (1969).
21 a) H.-J. Freund, C.-M. Liegener, Chem. Phys. Lett. 134, 70 (1987)
b) T. Porwol, Diplomarbeit, Ruhr-Universität Bochum (1989)
22 H. Siegbahn, L. Asplund, P. Kelfve, Chem. Phys. Lett. 35, 330 (1975)
23 E.U. Condon, G.H. Shortley "Theory of Atomic Spectra" (Cambridge University Press) (1935)
24 see for a discussion: W.F. Egelhoff, Surf.Sci.Rep. 6, 253 (1987).
25 J. Cooper, R.N. Zare "Photoelectron angular distributions" in Theoretical Physics, Vol. 11 c (Gordon and Breach, New York) p. 317 (1969)
26 M. J. Seaton, G. Peach, Proc. Phys. Soc. (London) 79, 1296 (1962).
27 a) B. Bartos, H.-J. Freund, H. Kuhlenbeck, M. Neumann, H. Lindner, K. Müller, Surf. Sci. 179, 59 (1987).
b) G. Illing, D. Heskett, E.W. Plummer, H.-J. Freund, J. Somers, Th. Lindner, A.M. Bradshaw, U. Buskotte, M. Neumann, U. Starke, K. Heinz, P. de Andres, D. Saldin, J. H. Pendry, Surf. Sci. 206, 1 (1988).
28 J.-H. Fock, H.-J. Lau, E.E. Koch, Chem. Phys. 83, 377 (1984).
29 H. Kuhlenbeck, M. Neumann, H.-J. Freund, Surf. Sci. 173, 194 (1986).
30 G. Illing, T. Porwol, I. Hemmerich, H. Kuhlenbeck, H.-J. Freund to be published
31 E. Umbach, Z. Hussain, Phys. Rev. Lett, 52, 754 (1984)
32 G. Dömötör, unpublished results.
33 K. Horn, J.N. Nardo, W. Eberhardt, H.-J. Freund, E.W. Plummer, Surf. Sci, 118, 465 (1982).
34 D. Saddei, H.-J. Freund, G. Hohlneicher, Surf. Sci. 95, 257 (1980)